Title

Towards cascading genetic risk in Alzheimers disease.

Permalink

Journal

Authors

Altmann, Andre
Aksman, Leon
Oxtoby, Neil
et al.

Publication Date

DOI

Peer reviewed

BRAIN
ORIGINAL ARTICLE

Towards cascading genetic risk in Alzheimer's disease

Andre Altmann,[1] Leon M. Aksman,[2] Neil P. Oxtoby,[3] Alexandra L. Young,[3] ADNI, Daniel C. Alexander,[3] Frederik Barkhof,[1,4,5] Maryam Shoai,[4,6] John Hardy[4,6] and Jonathan M. Schott[6,7]

See M-Carlgren (https://doi.org/10.1093/brain/awae237) for a scientific commentary on this article.

Alzheimer's disease typically progresses in stages, which have been defined by the presence of disease-specific biomarkers: amyloid (A), tau (T) and neurodegeneration (N). This progression of biomarkers has been condensed into the ATN framework, in which each of the biomarkers can be either positive (+) or negative (–). Over the past decades, genome-wide association studies have implicated ~90 different loci involved with the development of late-onset Alzheimer's disease. Here, we investigate whether genetic risk for Alzheimer's disease contributes equally to the progression in different disease stages or whether it exhibits a stage-dependent effect.

Amyloid (A) and tau (T) status was defined using a combination of available PET and CSF biomarkers in the Alzheimer's Disease Neuroimaging Initiative cohort. In 312 participants with biomarker-confirmed A–T– status, we used Cox proportional hazards models to estimate the contribution of *APOE* and polygenic risk scores (beyond *APOE*) to convert to A+T– status (65 conversions). Furthermore, we repeated the analysis in 290 participants with A+T– status and investigated the genetic contribution to conversion to A+T+ (45 conversions). Both survival analyses were adjusted for age, sex and years of education.

For progression from A–T– to A+T–, APOE-e4 burden showed a significant effect [hazard ratio (HR) = 2.88; 95% confidence interval (CI): 1.70–4.89; $P < 0.001$], whereas polygenic risk did not (HR = 1.09; 95% CI: 0.84–1.42; $P = 0.53$). Conversely, for the transition from A+T– to A+T+, the contribution of APOE-e4 burden was reduced (HR = 1.62; 95% CI: 1.05–2.51; $P = 0.031$), whereas the polygenic risk showed an increased contribution (HR = 1.73; 95% CI: 1.27–2.36; $P < 0.001$). The marginal *APOE* effect was driven by e4 homozygotes (HR = 2.58; 95% CI: 1.05–6.35; $P = 0.039$) as opposed to e4 heterozygotes (HR = 1.74; 95% CI: 0.87–3.49; $P = 0.12$).

The genetic risk for late-onset Alzheimer's disease unfolds in a disease stage-dependent fashion. A better understanding of the interplay between disease stage and genetic risk can lead to a more mechanistic understanding of the transition between ATN stages and a better understanding of the molecular processes leading to Alzheimer's disease, in addition to opening therapeutic windows for targeted interventions.

1 UCL Centre for Medical Image Computing, Department of Medical Physics and Biomedical Engineering, University College London, London, WC1E 6BT, UK
2 Stevens Neuroimaging and Informatics Institute, Keck School of Medicine, University of Southern California, Los Angeles, CA 90033, USA
3 UCL Centre for Medical Image Computing, Department of Computer Science, University College London, London, WC1E 6BT, UK
4 UCL Queen Square Institute of Neurology, University College London, London, WC1N 3BG, UK
5 Department of Radiology and Nuclear Medicine, Amsterdam University Medical Center, Amsterdam, 1081 HV, The Netherlands

6   UK Dementia Research Institute, University College London, London, WC1E 6BT, UK
7   Dementia Research Centre, UCL Queen Square Institute of Neurology, University College London, London, WC1N 3AR, UK

Correspondence to: Andre Altmann
90 High Holborn, 1st Floor, London, WC1V 6LJ, UK
E-mail: a.altmann@ucl.ac.uk

Introduction

Alzheimer's disease is characterized, at the neuropathological level, by the build-up of two proteins: amyloid plaques and neurofibrillary tangles of phosphorylated tau.[1] Both these pathological features can be observed long before the memory loss and decline in executive function that is characteristic of patients with Alzheimer's disease. Accumulation of amyloid plaques in the brain predates the clinical symptoms of Alzheimer's disease by two decades,[2] whereas the spatial distribution of tau tangles reflects more closely the reported cognitive deficits and neurodegeneration.[3]

The amyloid cascade hypothesis postulates that the deposition of the amyloid-β protein (the main component of the amyloid plaques) is the cause of Alzheimer's disease and that neurofibrillary tangles, cell loss, vascular damage and dementia are a direct consequence.[4] In keeping with the amyloid cascade hypothesis, a theoretical framework for the progression of biomarkers during the course of Alzheimer's disease has been developed.[5] Here, amyloid pathology is the first to appear, followed by tau pathology, neurodegeneration and, finally, cognitive decline. Support for this theoretical framework comes from a number of lines of evidence, including a variety of data-driven modelling approaches based on biomarker data.[6-10] In an attempt to operationalize this, a simplified ATN model has been proposed.[11] The components of the ATN model refer to the status of three different key biomarkers in Alzheimer's disease: amyloid (A), tau (T) and neurodegeneration (N). In this approach, each of the three biomarkers can be either positive or negative. Exceeding the centiloid threshold in amyloid PET imaging would place a participant into the A-positive (A+) group, whereas a scan slightly below the threshold would be considered amyloid negative (A−). One practical advantage (but also a major source of criticism) of this model is that the biomarker status can be assessed using a variety of methods: wet biomarkers (CSF or plasma) or brain imaging (centiloids or visual reads).[12] Although the progression from A−T−N− to A+T−N− to A+T+N− to A+T+N+ would be the most typical progression in Alzheimer's disease and in keeping with the theoretical framework of biomarker progression, all combinations of biomarker statuses emerge in observational cohorts.[13,14]

Genome-wide association studies (GWASs) have broadened the understanding of the genetic basis of late-onset Alzheimer's disease over the last decades.[15] Initially, these studies were restricted to cases with a clinical diagnosis of Alzheimer's disease and healthy controls.[16-18] Recently, these GWASs have been enriched with participants with a family history of Alzheimer's disease (diagnosis-by-proxy),[19-21] leading to a drastic increase in sample size and expanding the set of genetic risk loci for Alzheimer's disease to 90.[15] These loci have been linked to various molecular processes, such as immunity, cholesterol processing and endocytosis.[22]

Further studies investigated the genetic effects on Alzheimer's disease-related biomarkers, ranging from tau and amyloid levels in CSF[23,24] or in the brain[25,26] to MRI-based measures, such as hippocampal volume[27] and phenotypes derived from disease progression modelling.[28] The strongest common genetic risk factor for Alzheimer's disease is the e4 allele of the *APOE* gene: carriers of the e4 allele have a 2- to 4-fold increased risk of developing Alzheimer's disease, and e4 homozygous subjects have an 8- to 12-fold increased risk.[29] The genetic risk outside the *APOE* region is often summarized using polygenic scores, which have been shown to improve predictions of clinical diagnosis[30] and pathology-confirmed cases.[31] Likewise, the effect of *APOE* and the polygenic risk on various imaging and non-imaging biomarkers have been investigated,[32-35] with ongoing work suggesting that risk accumulated along different molecular pathways exerts differential effects on different biomarkers in Alzheimer's disease.[35-37]

For Alzheimer's disease and for other disorders, genetic risk is often considered as a time-invariant constant. That is, genetic risk identified through case–control studies is assumed to affect both onset and progression. However, given that Alzheimer's disease is now understood to unfold in stages, we hypothesized, in line with the amyloid cascade hypothesis and the A/T/N framework, that genetic risk in Alzheimer's disease is disease-stage dependent; i.e. some genetic risk factors will aid the transition from A− to A+, whereas other, distinct genetic risk factors will increase the risk to transition from T− to T+.

In this work, we explore whether genetic vulnerability to Alzheimer's disease varies with disease stage. Using longitudinal data from the Alzheimer's Disease Neuroimaging Imitative (ADNI) and survival analysis, we show that *APOE* contributes to progression from A−T− to A+T−, but only marginally from A+T− to A+T+. Conversely, polygenic risk contributes to the progression from A+T− to A+T+, but not from A−T− to A+T−.

Materials and methods

Data

Data used in the preparation of this article were obtained from the ADNI database (http://adni.loni.usc.edu). The ADNI was launched in 2003 as a public–private partnership, led by Principal Investigator Michael W. Weiner, MD. The primary goal of the ADNI has been to test whether serial MRI, PET, other biological markers, and clinical and neuropsychological assessment can be combined to measure the progression of mild cognitive impairment and early Alzheimer's disease. For up-to-date information, see https://adni.loni.usc.edu/about/. ADNI study data were accessed through the R package ADNIMERGE (accessed: 20 July 2023).

Preparation of genetic data

The genetic data preparation followed the procedure described by Altmann *et al.*[32] The additional genetic data contributed by the ADNI-3 cohort was integrated with the existing data using the same processing pipeline. Briefly, single nucleotide polymorphism (SNP) genotyping data were available for $n = 2001$ subjects across ADNI phases 1, 2, GO and 3. Genotyping was conducted using four different platforms: Human610-Quad, HumanOmniExpress, Omni 2.5 M and Illumina Infinium Global Screening Array v.2 (Illumina).[38] Prior to imputation, we applied subject-level quality control (QC) steps based on call rate (10% cut-off) and concordance between chip-inferred sex and self-reported sex separately for the four genotyping arrays; all subjects were retained. At the SNP level, we conducted standard QC steps ensuring compatibility with the reference panel used for imputation [strand consistency, allele names, position, reference/alternative allele assignments and minor allele frequency discrepancy (0.2 cut-off)]. Imputation was carried out using the Sanger Imputation Server (https://imputation.sanger.ac.uk/), with SHAPEIT for phasing,[39] positional Burrows–Wheeler transform[40] for imputation and the entire Haplotype Reference Consortium (release 1.1) reference panel.[41] Data from the four different genotyping platforms were imputed separately. As part of post-imputation QC, multi-allelic variants and SNPs with imputation INFO score of <0.3 were removed, and genotype calls with a posterior probability of <0.9 were set to missing (i.e. hard called). Following the initial QC, genotypes from the four platforms were merged. Additional information on the imputation and QC process is detailed by Scelsi *et al.*[28,42] Using the merged data, we retained SNPs with minor allele frequency ≥ 1% and genotyping rate of >0.9.

SNPweights[43] was used to infer genetic ancestry from genotyped SNPs. The reference panel comprised Central European, Yoruba Africans and East Asian samples from HapMap 3[44] and native Americans from Reich *et al.*[45] For this study, only participants with predicted central European ancestry of ≥80% were retained ($n = 1851$). Next, using the imputed and merged data genetic relatedness between central European participants was computed. Initially, the SNP content was restricted to SNPs with minor allele frequency ≥ 5%, and linkage disequilibrium (LD) pruning was carried out in PLINK v.1.9 (–indep-pairwise 1000 50 0.1). The genetic relatedness matrix was computed using the remaining autosomal SNPs, and the dataset was trimmed to remove subects with relatedness of >0.1 (–rel-cutoff 0.1), leading to $n = 1833$ unrelated participants.

Definition of genetic risk

In this study, we focused on two sources of genetic risk: (i) the risk conferred through the *APOE* gene based on the genetic markers for APOE-e2 and APOE-e4; and (ii) the polygenic risk conferred by the remaining genome. As described previously,[32] polygenic risk scores (PRSs) were computed using the software PRSice v.2.1.9.[46] As base GWAS, the stage 1 results of the Alzheimer's disease GWAS featuring a clinically defined Alzheimer's disease phenotype was used.[18] For PRS computation, SNPs with minor allele frequency ≥ 5% were considered, and SNPs were selected using LD clumping (1000 kb, R^2 of 0.1 and *P*-value threshold of 1.0) within the ADNI cohort, missing SNPs were simply ignored at the subject level (using the setting –missing SET_ZERO), and the *APOE* region was excluded (hg19 coordinates chr19 from 44 400 000 to 46 500 000). For this study, we used only the *P*-value cut-off of 1.0×10^{-8} to build the PRS (Supplementary Table 1). PRSs were computed for all ADNI

participants with genome-wide genotyping data. Of the remaining subjects, $n = 417$ ADNI-1 participants who contributed to the Alzheimer's disease GWAS[18] were excluded from the analysis to ensure independence between training and application dataset for PRS. Thus, $n = 1416$ unrelated participants with central European ancestry were eligible for inclusion in the study.

Definition of amyloid status

For this project we relied on two modalities to define amyloid status: amyloid-β PET using the ^{18}F-florbetapir and ^{18}F-florbetaben PET tracers, and CSF measures of amyloid-β(1–42) using the Roche Elecsys® immunoassay. We used data processed by ADNI for both modalities. Detailed information on the PET processing is available elsewhere (https://adni.loni.usc.edu/methods/pet–analysis)[47]; and information on CSF amyloid-β(1–42) processing is detailed by Bittner *et al.*[48] and Hansson *et al.*[49] For CSF amyloid-β(1–42) we used the cut-off of 880 pg/ml,[49] and for amyloid-β PET we used the tracer-specific standardized uptake value ratio (SUVR) (whole cerebellum reference) cut-offs of 1.11 and 1.08 for ^{18}F-florbetapir and the ^{18}F-florbetaben,[50] respectively.

A participant's visit was labelled as A+ if either the PET result or the CSF result indicated a positive amyloid finding (i.e. in cases where the results were discordant, the visit would be labelled as A+). Visits with only negative amyloid findings were labelled as A−, and visits without any information on amyloid (i.e. neither a PET nor a CSF result) were labelled as 'amyloid missing'.

Definition of tau status

In keeping with our definition of amyloid positivity, we used available data from CSF and PET imaging to define the tau status. More precisely, we used the Phospho-Tau(^{181}P) CSF Roche Elecsys® immunoassay and PET imaging using the ^{18}F-flortaucipir tracer. Details on the processing are available elsewhere (https://adni.loni.usc.edu/methods/pet–analysis).[48,49,51] For CSF we used phosphorylated ^{181}P tau (pTau) with a cut-off of 34.61 pg/ml, and for tau PET we used the cut-off of 1.42 in the meta temporal region of interest comprising the amygdala, entorhinal cortex, fusiform gyrus, inferior and middle temporal gyri[52] when normalized to the inferior cerebellar grey matter.[53] Both cut-offs were data driven: (i) the tau PET cut-off corresponds to a *z*-score of 2.0 in the cognitively normal participants in ADNI ($n = 506$) and is close to the 'high tau' cut-off of 1.43 defined by Jack Jr *et al.*[54]; and (ii) the pTau cut-off was set to maximize the Youden's index between CSF pTau and tau PET (at the 1.42 cut-off) in ($n = 502$) ADNI participants with concurrent CSF and PET measurements. The same labelling scheme as for amyloid was applied: a visit was labelled as T+ if either the CSF or the PET indicated a positive finding, T− if there were only negative tau findings, and 'tau missing' if neither data on CSF pTau nor on tau PET were available.

Statistical modelling

We used Cox proportional hazards models to investigate the genetic contribution of progressing (i) from A−T− to A+T−; and (ii) from A+T− to A+T+. For (i), we included every eligible participant with genetic data and who was A−T− based on their biomarker results as described above. This earliest A−T− visit was considered the 'start' visit (i.e. the status of previous visits was ignored). A subject was considered a converter when the available biomarkers indicated A+T− at a later visit. The time of the first A+T− biomarker finding after their initial A−T− visit was used as the conversion

time. For non-converters, we recorded the last visit where both amyloid and tau biomarker information was available to define the maximal follow-up time. Likewise, for (ii) we included every participant with genetic data and who was A+T−. This first A+T− visit was considered the 'start' visit. A subject was considered a converter when the available biomarkers indicated A+T+ at a later visit. The time of the first A+T+ biomarker finding after their initial A+T− visit was used as the conversion time. As before, for non-converters we recorded the last visit when amyloid and tau biomarker information was available as their last point of contact.

For the analyses, the Cox proportional hazards model included age at the inclusion visit (i.e. either the A−T− or the A+T− visit), sex and education. As variables of interest, we also included genetic variables for PRS, in addition to allele counts of APOE-e2 and APOE-e4. The proportional hazards assumption was tested for each covariate and for the global model using statistical tests and graphical diagnostics based on scaled Schoenfeld residuals. As a measure of overall model performance, the concordance index (C-index) was computed for the following: (i) full models; (ii) models without APOE; (iii) models without PRS; and (iv) models without any genetics. Statistical tests were carried out in R (v.4.1.0) using the survival (v.3.5.5), survminer (v.0.4.9) and rms (v.6.8.0) packages.

Sensitivity analyses

In addition to the two main analyses, we conducted a series of sensitivity analyses addressing the conversion definition, biomarker cut-offs, biomarker source and polygenic score source.

Conversion definition

To maximize the available data, we relaxed the requirement for both amyloid and tau biomarkers to be available at the same visit to define conversion. As before, both biomarkers at the same time were required to define the 'start' visit as either A−T− or A+T−. However, for defining progression from A−T− or A+T−, a single A+ or T+ visit was sufficient, respectively.

Biomarker cut-offs

We varied the tau PET cut-off from 1.0 to 3.0 standard deviations (SDs) above the mean in the cognitively normal ADNI participants. Notably, the lowest cut-off resulted in 1.31 and was close to the neuropathologically defined cut-off of 1.29 by Lowe et al.[55] The pTau cut-offs were adjusted accordingly to maximize Youden's index between CSF pTau and tau PET.

Biomarker source

To maximize data and follow-up time, the main analyses combined data from two biomarker sources: CSF and PET. Additional sensitivity analyses relied exclusively on either CSF biomarkers or PET biomarkers. For this analysis, pTau cut-offs were varied in the range from 22 to 31, covering the values of 24.25 and 29.19, which were found to indicate tau PET positivity in Braak III/IV and Braak V/VI regions, respectively.[56] Tau PET cut-offs were varied, as before, from 1.0 to 3.0 SD above the mean in cognitively normal participants (i.e. in the same range as the main analysis).

Polygenic score source

To include more SNPs in the PRS, we explored the summary statistics on Alzheimer's disease and related dementias by Bellenguez et al.[21] We followed the same PRS pipeline as above and applied a P-value threshold of 5.0×10^{-8} (i.e. genome-wide significant), leading to 77 included SNPs (Supplementary Table 2).

Results

Out of 16 401 visits recorded in ADNI, 3789 (23.1%) visits had both amyloid and tau biomarker data available. Concordance between PET- and CSF-based assessment was 80% and 81% for amyloid and tau, respectively. For both survival models, we identified ~300 subjects in the ADNI database with both biomarkers available (Table 1): 312 individuals were A−T−, of whom 65 converted to A+T−. The mean age of the A−T− group was 71.3 (6.65) years, and there was an almost equal number of males and females (49.4% females). Two hundred and ninety individuals were A+T− at any stage, of whom 45 converted to A+T+. The mean age of the A+T− group was 73.2 (6.9) years, significantly older than the A−T− group (Student's unpaired t-test: $t = 3.50$, $P < 0.001$). The fraction of females in that cohort was lower compared with the A−T− group (43.8% females), but not at a significant level (χ^2 test; $\chi^2 = 1.65$; d.f. = 1; $P = 0.19$). The distribution of APOE-e4 alleles (χ^2 test; $\chi^2 = 81.1$; d.f. = 2; $P = 2.4 \times 10^{-18}$) and APOE-e2 alleles (Fisher's exact test; $P = 0.0004$) differed significantly between A−T− and A+T−. There were more APOE-e2 carriers and fewer APOE-e4 carriers in the A−T− group than in the A+T− group. The PRS did not differ between the A−T− and A+T− groups (Student's two-tailed t-test; $t = 0.84$; d.f. = 600; $P = 0.39$). The cohort with the relaxed conversion criterion showed comparable characteristics (Supplementary Table 3).

Table 1 Demographics

Characteristic	A−T−			A+T−		
	Total	Stable	Converter	Total	Stable	Converter
n	312	247	65	290	245	45
Age, mean (SD), years	71.3 (6.65)	71.0 (6.47)	72.2 (7.25)	73.2 (6.9)	73.2 (6.9)	73.1 (6.8)
Sex (% female)	49.4	48.6	52.3	43.8	43.3	46.7
Diagnosis (CN/MCI/AD)	195/113/4	150/94/3	45/19/1	118/153/19	100/128/17	18/25/2
Education, mean (SD), years	16.7 (2.5)	16.6 (2.6)	17.3 (2.2)	16.4 (2.6)	16.6 (2.7)	15.5 (2.4)
Follow-up, mean (SD), years	5.0 (3.1)	4.7 (3.0)	6.4 (3.4)	4.1 (2.6)	3.8 (2.6)	5.6 (2.3)
Time to event, mean (SD), years	n/a	n/a	4.5 (2.7)	n/a	n/a	4.4 (2.5)
APOE-e4 (0/1/2)	252/57/3	207/40/0	45/17/3	137/119/34	121/99/25	16/20/9
APOE-e2 (0/1/2)	265/46/1	205/41/1	60/5/0	273/17/0	230/15/0	43/2/0
PRS, mean (SD)	0.013 (0.012)	0.013 (0.012)	0.013 (0.011)	0.013 (0.013)	0.012 (0.013)	0.020 (0.011)

AD = Alzheimer's disease; CN = cognitively normal; MCI = mild cognitive impairment; PRS = polygenic risk score.
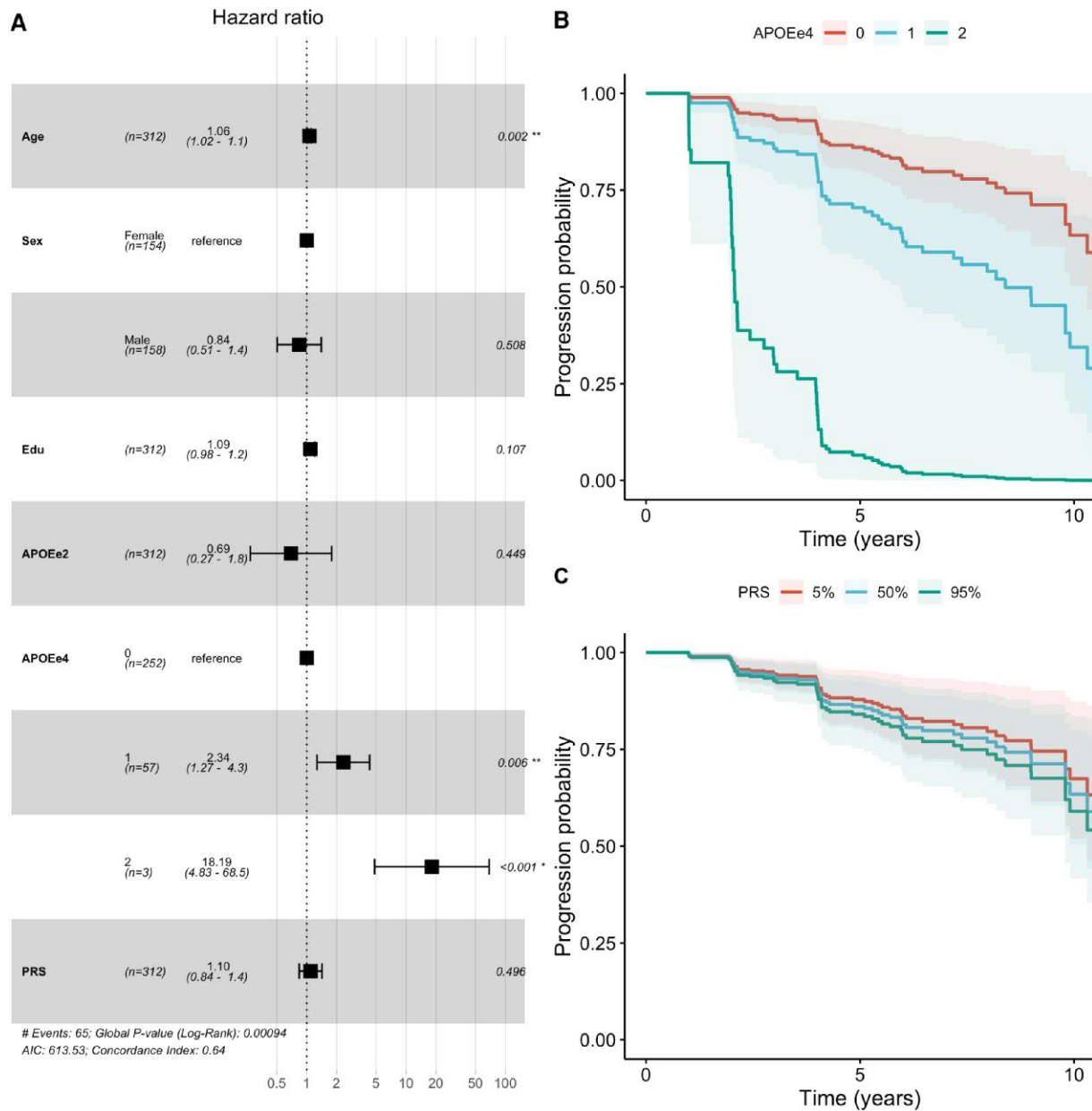
Figure 1 Hazard ratios for the conversion from A−T− to A+T−. (**A**) Forest plot depicting the HRs for all covariates in the model. (**B**) Estimated survival curves stratified by APOE-e4 genotype. (**C**) Estimated survival curves stratified by PRS percentile (5%, 50% and 95%). APOEe2 = number of APOE-e2 alleles; APOEe4 = number of APOE-e4 alleles; Edu = years of education; HR = hazard ratio; PRS = polygenic risk score, scaled to zero mean and unit standard deviation.

APOE-e4 influences progression from A−T− to A+T−

The survival analysis showed a significant contribution by APOE-e4 allele count [hazard ratio (HR) = 2.88; 95% confidence interval (CI): 1.70–4.89; $P = 8.7 \times 10^{-5}$] but no significant contribution by PRS (HR = 1.09; 95% CI: 0.84–1.42; $P = 0.53$) (Fig. 1). The APOE-e2 allele count directionally favoured a protective effect, but this was not significant (HR = 0.73; 95% CI: 0.28–1.86; $P = 0.51$). The Cox proportional hazards assumption held for this model (global Schoenfeld test, $P = 0.24$) (Supplementary Fig. 1). The C-indices aligned with this pattern: full model (C = 0.612), no *APOE* (C = 0.525), no PRS (C = 0.611) and no genetics (C = 0.531). This pattern of associations of *APOE* and PRS with progression was largely independent of the tau PET and pTau thresholds (Supplementary Table 4).

Furthermore, using the more relaxed conversion criteria (i.e. confirmed A+ status was sufficient instead of a confirmation of A+T−) yielded more conversions (85 instead of 65), but qualitatively the same result (Supplementary Fig. 2), i.e. a significant contribution by APOE-e4 allele count (HR = 3.34; 95% CI: 2.14–5.22; $P = 1.0 \times 10^{-7}$) but not by PRS (HR = 1.06; 95% CI: 0.84–1.34; $P = 0.61$).

Polygenic risk affects the progression from A+T− to A+T+

The survival analysis showed a marginally significant contribution by APOE-e4 burden (HR = 1.62; 95% CI: 1.05–2.51; $P = 0.031$), which was mainly driven by APOE-e4 homozygotes (HR = 2.58; 95% CI: 1.05–6.35; $P = 0.039$) rather than APOE-e4 heterozygotes (HR = 1.74;
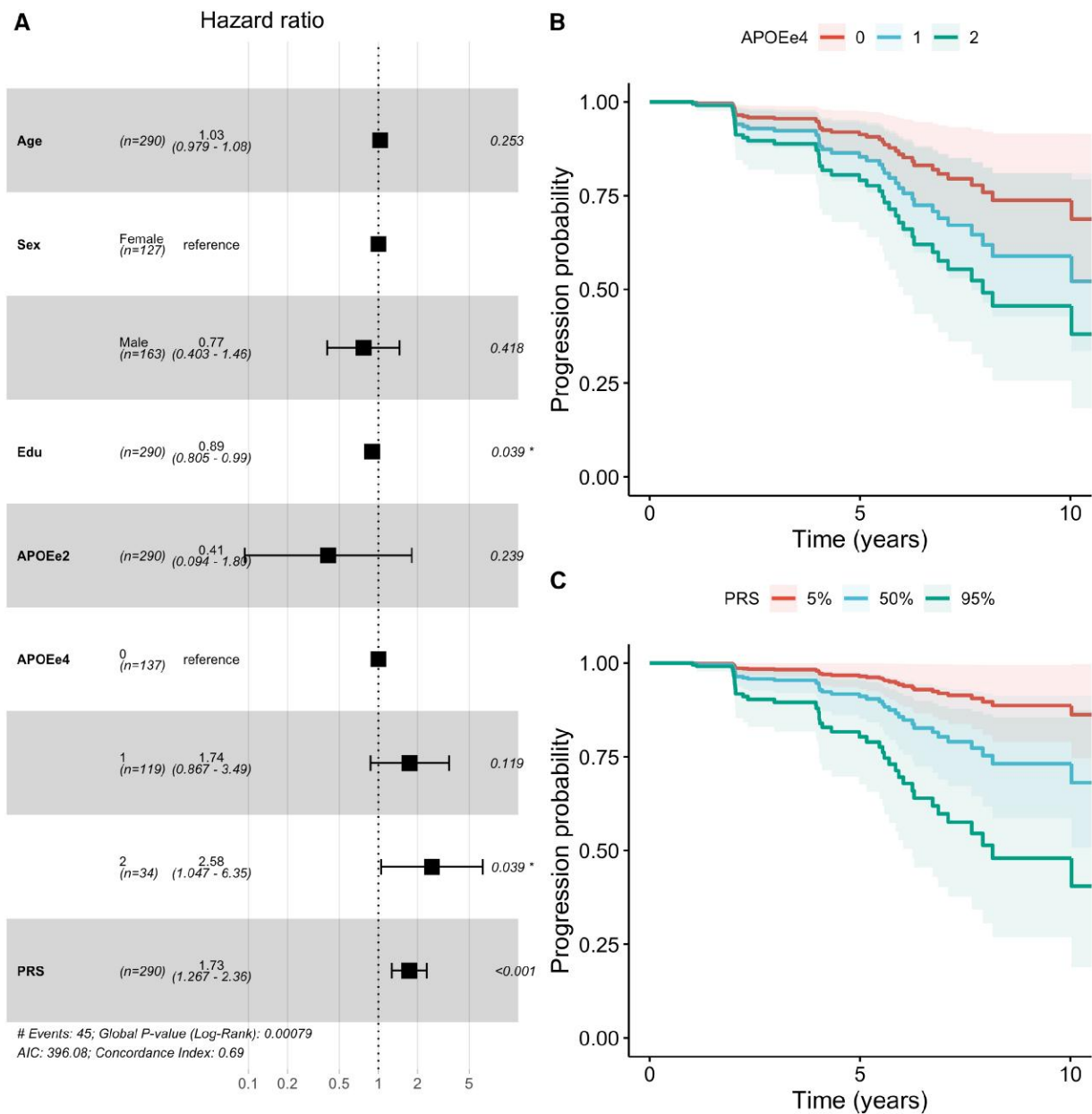
Figure 2 Hazard ratios for the conversion from A+T− to A+T+. (**A**) Forest plot depicting the hazard ratios for all covariates in the model. (**B**) Estimated survival curves stratified by APOE-e4 genotype. (**C**) Estimated survival curves stratified by PRS percentile (5%, 50% and 95%). APOEe2 = number of APOE-e2 alleles; APOEe4 = number of APOE-e4 alleles; Edu = years of education; PRS = polygenic risk score, scaled to zero mean and unit standard deviation.

95% CI: 0.87–3.49; P = 0.12) (Fig. 2). Furthermore, there was a significant contribution by PRS (HR = 1.72; 95% CI: 1.27–2.36; P = 0.00057). The APOE-e2 allele count again was directionally consistent with a protective effect, but this was not significant (HR = 0.41; 95% CI: 0.09–1.78; P = 0.23). The Cox proportional hazards assumption held for this model (Supplementary Fig. 3). The C-indices dropped marginally when either *APOE* or PRS was removed from the model: full model (C = 0.657), no *APOE* (C = 0.634), no PRS (C = 0.615) and no genetics (C = 0.549). Moreover, the association pattern of *APOE* and PRS with progression was largely independent of the tau PET and pTau cut-offs (Supplementary Table 4). In addition, education showed a marginally protective association with conversion to A+T+ (HR = 0.89; 95% CI: 0.80–0.99; P = 0.039). Applying the more

relaxed conversion criteria (i.e. confirmed T+ status was sufficient instead of a confirmation of A+T+) yielded more conversions (51 instead of 45), but qualitatively the same result (Supplementary Fig. 4): a significant contribution by PRS (HR = 1.62; 95% CI: 1.22–2.17; P = 0.001) and a marginal contribution by APOE-e4 allele burden (HR = 1.56; 95% CI: 1.04–2.35; P = 0.031).

Results are independent of PRS source

Using an the alternative PRS with 77 SNPs led to the same observation of a significant effect by APOE-e4 burden on A−T− to A+T− conversion (HR = 2.84; 95% CI: 1.68–4.82; P = 0.0001) and a lack of contribution by the PRS (HR = 0.97; 95% CI: 0.77–1.2; P = 0.80;
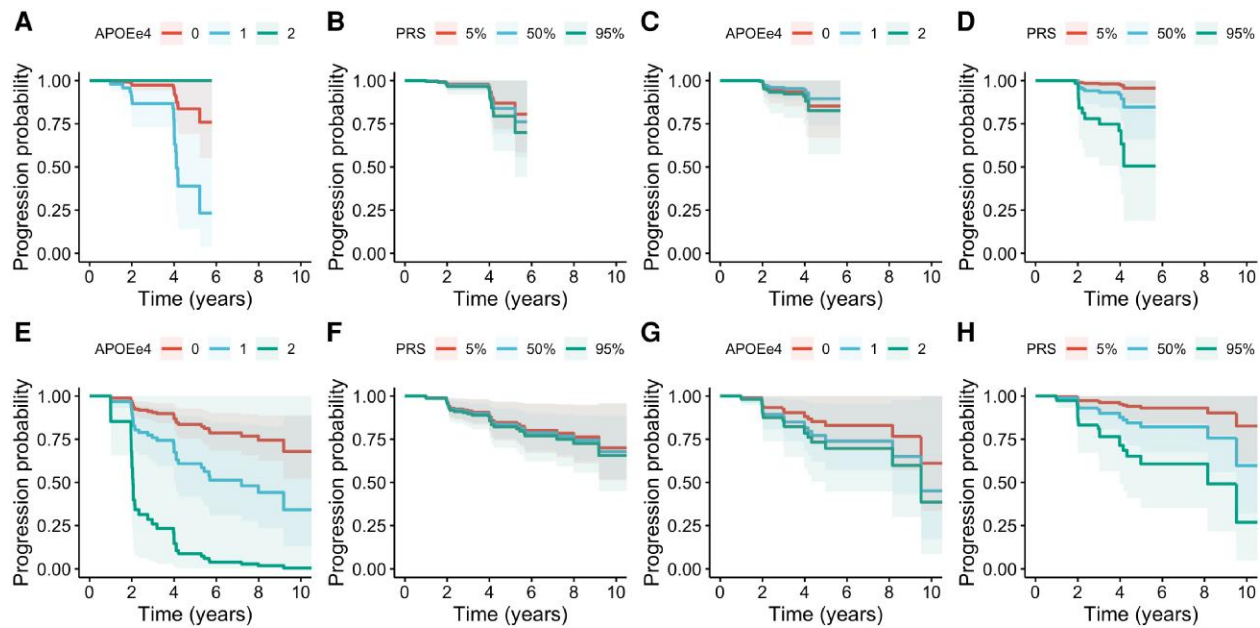
Figure 3 Survival curves for PET-only and CSF-only analyses. The *top row* (**A–D**) is based on results from AT(N) definitions based exclusively on PET biomarkers (amyloid and tau), with a cut-off of 1.45 for tau PET. The *bottom row* (**E–H**) relied on CSF biomarkers (ABETA42 and pTAU), with a cut-off of 26 for pTau. The *two left columns* (**A, B, E** and **F**) display the progression probability from A–T– to A+T– stratified by APOE-e4 genotype and PRS quantile (5%, 50% and 95%). The *two right columns* (**C, D, G** and **H**) display the progression probability from A+T– to A+T+.

Supplementary Fig. 5A). Conversely, for A+T– to A+T+ conversion, the contribution by APOE-e4 was reduced (HR = 1.71; 95% CI: 1.09–2.68; P = 0.019), whereas the PRS exhibited a strong contribution (HR = 1.59; 95% CI: 1.19–2.13; P = 0.00163; Supplementary Fig. 5B).

Results are independent of biomarker source

The main analysis combined different biomarker sources to maximize the available data and the observation time for the conversion analysis. Relying on PET biomarkers alone, only 7.5% of visits (1237 of 16 401) had both biomarkers, and it resulted in shorter observation times for A–T– to A+T– conversion [3.62 (SD = 1.07) years] and A+T– to A+T+ conversion [2.94 (SD = 1.13) years] compared with the main analysis. Relying solely on CSF biomarkers, 19.2% of visits (3155 of 16 401) had both biomarkers. Overall, this led to a shorter observation time with respect to the main analysis for A–T– to A+T– conversion [3.94 (SD = 2.7) years] and A+T– to A+T+ conversions [3.6 (SD = 2.38) years]. Furthermore, relying on a single source of biomarkers led to reduced sample sizes (from ∼300 in the main analyses to 70–250 in the sensitivity analyses) and observed conversions (Supplementary Tables 5 and 6). Despite the reduced statistical power, these sensitivity analyses confirmed the pattern observed in the main analysis: APOE-e4 contributed mainly to the A–T– to A+T– conversion, whereas PRS contributed to the A+T– to A+T+ conversion (Fig. 3 and Supplementary Tables 5 and 6).

Discussion

This longitudinal survival analysis demonstrated that APOE-e4 plays an important role for the progression from A–T– to A+T–, but *APOE* is of only marginal importance in A+T– participants who progress to A+T+. Conversely, polygenic risk for Alzheimer's disease exhibited the inverse pattern: there was no contribution to the progression from A–T– to A+T–, but a significant contribution to faster progression from A+T– to A+T+. This held true for

an alternative PRS defined using a different genetic study and involving a larger number of genetic loci. Notably, when assessing covariates, a differential effect of years of education was observed: higher education had no effect (Fig. 1) or was marginally harmful (Supplementary Fig. 2) for the progression from A–T– to A+T– but was protective for the conversion from A+T– to A+T+ (Fig. 2). The bisection of the genetic risk by disease stage was largely independent of the applied biomarker cut-offs. Moreover, relying on only a single source of biomarkers for defining stage and conversion confirmed the findings of the main analysis despite reduced sample size and observation time.

The finding of a stronger effect of APOE-e4 earlier in the disease progress might explain the observation of stronger genetic effect of APOE-e4 on Alzheimer's disease in the group of 60- to 80-year-old people compared with people ≥80 years old.[57-59] Given that amyloid deposition occurs 10+ years before other Alzheimer's disease processes[2] and APOE-e4 is the strongest common genetic risk factor for amyloid deposition, it would be expected for APOE-e4 to exert its maximum effect in younger people. Still, *APOE* remains the strongest risk factor in individuals ≥80 years old.[58] Thus, the age-dependent heterogeneity of *APOE* is likely to be compounded by a survivor bias: individuals with a very late onset despite carrying APOE-e4 might harbour protective variants,[60] such as KLOTHO-VS, where a protective effect on amyloid deposition and Alzheimer's disease was observed in only 60- to 80-year-olds, but not in the 80+ group.[57,61]

The findings from this longitudinal analysis are also in line with previous reports in the ADNI cohort of *APOE* and polygenic risk on amyloid and tau. For instance, cross-sectional amyloid biomarkers in the CSF and in the brain were mainly driven by *APOE*, whereas cross-sectional CSF tTau and pTau measurements were associated with PRS beyond the *APOE* locus.[32] Moreover, *APOE* was found to predict amyloid status, whereas polygenic risk for Alzheimer's disease improved predictions of diagnosis and of clinical progression from mild cognitive impairment to Alzheimer's disease above

APOE alone.[35] These observations extend to plasma markers of tau pathology: PRSs (that excluded the *APOE* region) were found to be associated only with plasma p-tau181 in A+ participants.[62] This association between polygenic risk (beyond *APOE*) and CSF tau biomarkers rather than with amyloid and neurodegeneration was also observed outside of the ADNI study.[63] Polygenic risk (beyond *APOE*) was associated with non-amyloid endophenotypes in a large cohort of people with mild cognitive impairment. This suggests that these variants are more closely linked with neuronal degeneration than with Alzheimer's disease-related amyloid pathology.[64] All these previous studies made the connection between existing amyloid pathology and correlations between polygenic risk and tau pathology using cross-sectional study designs. In a recent longitudinal study of tau PET in the ADNI cohort, higher polygenic risk for Alzheimer's disease was associated with accelerated increase in tau signal in the brain, and this effect was modulated by amyloid pathology: A+ participants showed a stronger effect of PRS on tau accumulation.[65] Our longitudinal analysis, which combined CSF and PET data to maximize the sample size, confirms these observations and indicates that polygenic Alzheimer's disease risk (outside the *APOE* region) contributes to tau pathology in A+ participants but has no meaningful contribution in A− participants. The genetic architecture of Alzheimer's disease, as captured by the PRS, involves multiple different pathways, mainly amyloid-β processing, tau, immunity and lipid processing.[18,21] The PRS that we used covers three genes that have been associated with tau binding: *BIN1*, *CLU* and *PICALM*. *BIN1* mediates Alzheimer's disease risk by modulating tau pathology,[66] and *BIN1* risk variants increase tau PET (but not amyloid PET)[67] in an amyloid-dependent fashion.[68] Our observations of an amyloid-dependent effect of the PRS align with these earlier single-gene studies. Although there are currently no mechanistic analyses that explain the amyloid-dependent effect of *BIN1* on tau pathology, recent data from animal models in Alzheimer's disease suggest a state-dependent effect of genetic risk factors related to microglia: deletion of *Trem2* in mouse models exacerbated tau accumulation and spreading, leading to brain atrophy, but only in the presence of existing amyloid-β pathology.[69] Along the same lines, physical contact between microglia and plaques in addition to a functioning *TREM2* gene are necessary for the appropriate microglial response to amyloid pathology.[70] Thus, defects in *TREM2* can contribute to neurodegeneration only once amyloid pathology has been established. Consequently, other genes contributing to the PRS might also exert their effect in an amyloid-dependent fashion. Our longitudinal analysis presented here is the first to support such a state-dependent genetic risk model in humans, and further fine-grained examination of how the pathways involved in the PRS contribute to sequential disease progression are needed.

The partition of Alzheimer's disease genetic risk into *APOE*-related and polygenic risk beyond *APOE* is a simplification in this analysis. Recent works have linked established Alzheimer's disease risk loci outside *APOE*, such as *CR1*, to amyloid biomarker levels.[23] Conversely, studies of biomarker levels of tau repeatedly highlight the *APOE* locus.[23,24] However, if being A+ were a prerequisite to exhibit pathological accumulation of tau, then the strong genetic association with *APOE* in these GWASs would merely reflect the necessary condition rather than a genuine direct molecular process that affects tau levels. The strong dependence of tau levels on established amyloid pathology is supported by mediation analyses in recent cross-sectional[63] and longitudinal[65] studies. Moreover, the known Alzheimer's disease genetic risk variants are contributing differently to molecular pathways,[18,21,22] where each pathway

in turn will exercise differential effects on the Alzheimer's disease biomarkers, including markers for vascular pathology.[37] Therefore, a pathway PRS comprising only genes associated with the regulation of the amyloid precursor protein catabolic process (e.g. Gene Ontology term GO:1902991) might contribute significantly to the conversion from A−T− to A+T−. Likewise, a pathway PRS using only genes known to bind the tau protein (GO:0048156) might exhibit an even stronger association with A+T− to A+T+ conversion than the general PRS used here.

In addition to the cascading effect of genetic risk in Alzheimer's disease, we also observed a stage-dependent effect of non-genetic risk factors. Education has been shown to have a protective effect against dementia[71]: here, we show that higher rates of education do not influence transition to amyloid positivity but do slow progression from A+T− to A+T+. Consequently, other non-genetic risk factors might show a similarly state-dependent effect on the pathological pathway from A−T− to A+T+ and further neurodegeneration.

The study has several limitations. First, the present analysis was limited to two biomarkers in Alzheimer's disease: amyloid-β and tau. It would be desirable to include neurodegeneration (N; of the ATN framework) or, potentially, more fine-grade staging from advanced data-driven disease-progression modelling.[7] However, at this point adding further stages would reduce the available sample size. Second, we partitioned the genetic risk in Alzheimer's disease into two components: *APOE* and other top variants combined into a single polygenic risk score. Further work should explore a more fine-grained partition of the polygenic risk into individual SNPs or into pathway PRS.[37] Third, the study population was of central European ancestry; therefore, it is unclear whether the findings would generalize to other genetic backgrounds. Finally, although the ADNI cohort is a large cohort, the number of subjects who were eligible for our analysis was reduced owing to the requirement for concordant and longitudinal recordings of multiple biomarkers in addition to genetics. The available sample size might have limited statistical power to render the estimated hazards ratios significant in some settings. However, the two conversion analyses were based on similar sample sizes (~300 participants), thus allowing us to make a relative comparison between the genetic effect (of *APOE* or PRS) under two different biomarker-defined disease stages. Moreover, uncertainty of the estimated effects might also be increased owing to disease heterogeneity in Alzheimer's disease,[72-75] which is likely to be underpinned by differences in genetic architecture. Thus, analyses in further large longitudinal cohorts are required to confirm the observation of stage-dependent genetic vulnerability in Alzheimer's disease and to uncover more fine-grained associations with Alzheimer's disease subtypes.

Conclusion

In this work we demonstrated, in a simplified setting, that genetic risk for late-onset Alzheimer's disease unfolds in a disease stage-dependent fashion. A better understanding of the interplay between disease stage and genetic risk can lead to a better understanding of the molecular processes leading to Alzheimer's disease, in addition to opening therapeutic windows for targeted interventions and personalized approaches to dementia prevention.

Data availability

Data used in the preparation of this article were obtained from the ADNI database (http://adni.loni.usc.edu) and are freely available

after registration. Analysis scripts are available at: https://github.com/andrealtmann/cascading_genetic_risk.

Competing interests

The authors report no competing interests.

Supplementary material

Supplementary material is available at *Brain* online.

References

1. Braak H, de Vos RAI, Jansen ENH, Bratzke H, Braak E. Neuropathological hallmarks of Alzheimer's and Parkinson's diseases. *Prog Brain Res*. 1998;117:267-285.
2. Bateman RJ, Xiong C, Benzinger TLS, et al. Clinical and biomarker changes in dominantly inherited Alzheimer's disease. *N Engl J Med*. 2012;367:795-804.
3. Ossenkoppele R, Schonhaut DR, Schöll M, et al. Tau PET patterns mirror clinical and neuroanatomical variability in Alzheimer's disease. *Brain*. 2016;139(Pt 5):1551-1567.
4. Selkoe DJ, Hardy J. The amyloid hypothesis of Alzheimer's disease at 25 years. *EMBO Mol Med*. 2016;8:595-608.
5. Jack CR Jr, Knopman DS, Jagust WJ, et al. Tracking pathophysiological processes in Alzheimer's disease: An updated hypothetical model of dynamic biomarkers. *Lancet Neurol*. 2013;12:207-216.
6. Fonteijn HM, Modat M, Clarkson MJ, et al. An event-based model for disease progression and its application in familial Alzheimer's disease and Huntington's disease. *Neuroimage*. 2012;60:1880-1889.
7. Young AL, Oxtoby NP, Daga P, et al. A data-driven model of biomarker changes in sporadic Alzheimer's disease. *Brain*. 2014;137(Pt 9):2564-2577.
8. Donohue MC, Jacqmin-Gadda H, Le Goff M, et al. Estimating long-term multivariate progression from short-term data. *Alzheimers Dement*. 2014;10(5 Suppl):S400-S410.
9. Jedynak BM, Lang A, Liu B, et al. A computational neurodegenerative disease progression score: Method and results with the Alzheimer's disease neuroimaging initiative cohort. *Neuroimage*. 2012;63:1478-1486.
10. Lorenzi M, Filippone M, Frisoni GB, et al. Probabilistic disease progression modeling to characterize diagnostic uncertainty: Application to staging and prediction in Alzheimer's disease. *Neuroimage*. 2019;190:56-68.
11. Jack CR Jr, Bennett DA, Blennow K, et al. NIA-AA research framework: Toward a biological definition of Alzheimer's disease. *Alzheimers Dement*. 2018;14:535-562.
12. van der Flier WM, Scheltens P. The ATN framework—Moving preclinical Alzheimer disease to clinical relevance. *JAMA Neurol*. 2022;79:968-970.
13. Ebenau JL, Timmers T, Wesselman LMP, et al. ATN classification and clinical progression in subjective cognitive decline: The SCIENCe project. *Neurology*. 2020;95:e46-e58.
14. Ingala S, De Boer C, Masselink LA, et al. Application of the ATN classification scheme in a population without dementia: Findings from the EPAD cohort. *Alzheimers Dement*. 2021;17:1189-1204.
15. Lambert JC, Ramirez A, Grenier-Boley B, Bellenguez C. Step by step: Towards a better understanding of the genetic architecture of Alzheimer's disease. *Mol Psychiatry*. 2023;28:2716-2727.
16. Hollingworth P, Harold D, Sims R, et al. Common variants at *ABCA7*, *MS4A6A/MS4A4E*, *EPHA1*, *CD33* and *CD2AP* are associated with Alzheimer's disease. *Nat Genet*. 2011;43:429-435.
17. Lambert JC, Ibrahim-Verbaas CA, Harold D, et al. Meta-analysis of 74,046 individuals identifies 11 new susceptibility loci for Alzheimer's disease. *Nat Genet*. 2013;45:1452-1458.
18. Kunkle BW, Grenier-Boley B, Sims R, et al. Genetic meta-analysis of diagnosed Alzheimer's disease identifies new risk loci and implicates Aβ, tau, immunity and lipid processing. *Nat Genet*. 2019;51:414-430.
19. Jansen IE, Savage JE, Watanabe K, et al. Genome-wide meta-analysis identifies new loci and functional pathways influencing Alzheimer's disease risk. *Nat Genet*. 2019;51:404-413.
20. Wightman DP, Jansen IE, Savage JE, et al. A genome-wide association study with 1,126,563 individuals identifies new risk loci for Alzheimer's disease. *Nat Genet*. 2021;53:1276-1282.
21. Bellenguez C, Küçükali F, Jansen IE, et al. New insights into the genetic etiology of Alzheimer's disease and related dementias. *Nat Genet*. 2022;54:412-436.
22. Sims R, Hill M, Williams J. The multiplex model of the genetics of Alzheimer's disease. *Nat Neurosci*. 2020;23:311-322.
23. Jansen IE, van der Lee SJ, Gomez-Fonseca D, et al. Genome-wide meta-analysis for Alzheimer's disease cerebrospinal fluid biomarkers. *Acta Neuropathol*. 2022;144:821-842.
24. Deming Y, Li Z, Kapoor M, et al. Genome-wide association study identifies four novel loci associated with Alzheimer's endophenotypes and disease modifiers. *Acta Neuropathol*. 2017;133:839-856.
25. Yan Q, Nho K, Del-Aguila JL, et al. Genome-wide association study of brain amyloid deposition as measured by Pittsburgh Compound-B (PiB)-PET imaging. *Mol Psychiatry*. 2021;26:309-321.
26. Ramanan VK, Wang XK, Przybelski SA, et al. Genome-wide association study of tau-PET: Association of variant near NTNG2

with resistance to tau deposition: Neuroimaging: Imaging genetics. *Alzheimers Dement.* 2020;16:e044321.

27. Hibar DP, Adams HHH, Jahanshad N, et al. Novel genetic loci associated with hippocampal volume. *Nat Commun.* 2017;8:13624.

28. Scelsi MA, Khan RR, Lorenzi M, et al. Genetic study of multimodal imaging Alzheimer's disease progression score implicates novel loci. *Brain.* 2018;141:2167-2180.

29. Belloy ME, Napolioni V, Greicius MD. A quarter century of APOE and Alzheimer's disease: Progress to date and the path forward. *Neuron.* 2019;101:820-838.

30. Escott-Price V, Sims R, Bannister C, et al. Common polygenic variation enhances risk prediction for Alzheimer's disease. *Brain.* 2015;138:3673-3684.

31. Escott-Price V, Myers AJ, Huentelman M, Hardy J. Polygenic risk score analysis of pathologically confirmed Alzheimer disease. *Ann Neurol.* 2017;82:311-314.

32. Altmann A, Scelsi MA, Shoai M, et al. A comprehensive analysis of methods for assessing polygenic burden on Alzheimer's disease pathology and risk beyond *APOE*. *Brain Commun.* 2020;2: fcz047.

33. Sabuncu MR, Buckner RL, Smoller JW, et al. The association between a polygenic Alzheimer score and cortical thickness in clinically normal subjects. *Cereb Cortex.* 2012;22:2653-2661.

34. Mormino EC, Sperling RA, Holmes AJ, et al. Polygenic risk of Alzheimer disease is associated with early- and late-life processes. *Neurology.* 2016;87:481-488.

35. Leonenko G, Shoai M, Bellou E, et al. Genetic risk for Alzheimer's disease is distinct from genetic risk for amyloid deposition. *Ann Neurol.* 2019;86:427-435.

36. Darst BF, Koscik RL, Racine AM, et al. Pathway-specific polygenic risk scores as predictors of amyloid-β deposition and cognitive function in a sample at increased risk for Alzheimer's disease. *J Alzheimers Dis.* 2017;55:473-484.

37. Lorenzini L, Collij LE, Tesi N, et al. Alzheimer's disease genetic pathways impact on cerebrospinal fluid biomarkers and imaging endophenotypes in non-demented individuals. *Alzheimer's Dement.* 2024; (in press).

38. Saykin AJ, Shen L, Foroud TM, et al. Alzheimer's Disease Neuroimaging Initiative biomarkers as quantitative phenotypes: Genetics core aims, progress, and plans. *Alzheimers Dement.* 2010;6:265-273.

39. Delaneau O, Zagury JF, Marchini J. Improved whole-chromosome phasing for disease and population genetic studies. *Nat Methods.* 2013;10:5-6.

40. Durbin R. Efficient haplotype matching and storage using the positional Burrows–Wheeler transform (PBWT). *Bioinformatics.* 2014;30:1266-1272.

41. McCarthy S, Das S, Kretzschmar W, et al. A reference panel of 64,976 haplotypes for genotype imputation. *Nat Genet.* 2016;48: 1279-1283.

42. Scelsi MA, Altmann A. The hitchhiker's guide to GWAS. Accessed 17 July 2024. https://rpubs.com/maffleur/452627

43. Chen CY, Pollack S, Hunter DJ, Hirschhorn JN, Kraft P, Price AL. Improved ancestry inference using weights from external reference panels. *Bioinformatics.* 2013;29:1399-1406.

44. International HapMap 3 Consortium; Altshuler DM, Gibbs RA, et al. Integrating common and rare genetic variation in diverse human populations. *Nature.* 2010;467:52-58.

45. Reich D, Patterson N, Campbell D, et al. Reconstructing Native American population history. *Nature.* 2012;488:370-374.

46. Euesden J, Lewis CM, O'Reilly PF. PRSice: Polygenic risk score software. *Bioinformatics.* 2015;31:1466-1468.

47. Landau SM, Breault C, Joshi AD, et al. Amyloid-β imaging with Pittsburgh compound B and florbetapir: Comparing radiotracers and quantification methods. *J Nucl Med.* 2013;54:70-77.

48. Bittner T, Zetterberg H, Teunissen CE, et al. Technical performance of a novel, fully automated electrochemiluminescence immunoassay for the quantitation of β-amyloid (1–42) in human cerebrospinal fluid. *Alzheimers Dement.* 2016;12: 517-526.

49. Hansson O, Seibyl J, Stomrud E, et al. CSF biomarkers of Alzheimer's disease concord with amyloid-β PET and predict clinical progression: A study of fully automated immunoassays in BioFINDER and ADNI cohorts. *Alzheimers Dement.* 2018;14: 1470-1481.

50. Royse SK, Minhas DS, Lopresti BJ, et al. Validation of amyloid PET positivity thresholds in centiloids: A multisite PET study approach. *Alzheimers Res Ther.* 2021;13:99.

51. Maass A, Landau S, Baker SL, et al. Comparison of multiple tau-PET measures as biomarkers in aging and Alzheimer's disease. *Neuroimage.* 2017;157:448-463.

52. Jack CR Jr, Wiste HJ, Weigand SD, et al. Defining imaging biomarker cut points for brain aging and Alzheimer's disease. *Alzheimers Dement.* 2017;13:205-216.

53. Diedrichsen J. A spatially unbiased atlas template of the human cerebellum. *Neuroimage.* 2006;33:127-138.

54. Jack CR Jr, Wiste HJ, Algeciras-Schimnich A, et al. Predicting amyloid PET and tau PET stages with plasma biomarkers. *Brain.* 2023;146:2029-2044.

55. Lowe VJ, Lundt ES, Albertson SM, et al. Tau-positron emission tomography correlates with neuropathology findings. *Alzheimers Dement.* 2020;16:561-571.

56. Leuzy A, Janelidze S, Mattsson-Carlgren N, et al. Comparing the clinical utility and diagnostic performance of CSF P-Tau181, P-Tau217, and P-Tau231 assays. *Neurology.* 2021;97:e1681-e1694.

57. Belloy ME, Napolioni V, Han SS, Le Guen Y, Greicius MD; Alzheimer's Disease Neuroimaging Initiative. Association of *Klotho*-VS heterozygosity with risk of Alzheimer disease in individuals who carry APOE4. *JAMA Neurol.* 2020;77:849-862.

58. Lo MT, Kauppi K, Fan CC, et al. Identification of genetic heterogeneity of Alzheimer's disease across age. *Neurobiol Aging.* 2019; 84:243.e1-243.e9.

59. Jansen WJ, Ossenkoppele R, Knol DL, et al. Prevalence of cerebral amyloid pathology in persons without dementia: A meta-analysis. *JAMA.* 2015;313:1924-1938.

60. Bonham LW, Geier EG, Fan CC, et al. Age-dependent effects of *APOE* ε4 in preclinical Alzheimer's disease. *Ann Clin Transl Neurol.* 2016;3:668-677.

61. Belloy ME, Eger SJ, Le Guen Y, et al. *KL*∗VS heterozygosity reduces brain amyloid in asymptomatic at-risk *APOE*∗4 carriers. *Neurobiol Aging.* 2021;101:123-129.

62. Zettergren A, Lord J, Ashton NJ, et al. Association between polygenic risk score of Alzheimer's disease and plasma phosphorylated tau in individuals from the Alzheimer's Disease Neuroimaging Initiative. *Alzheimers Res Ther.* 2021;13:17.

63. Kumar A, Janelidze S, Stomrud E, et al. β-Amyloid-dependent and -independent genetic pathways regulating CSF tau biomarkers in Alzheimer disease. *Neurology.* 2022;99:e476-e487.

64. Louwersheimer E, Wolfsgruber S, Espinosa A, et al. Alzheimer's disease risk variants modulate endophenotypes in mild cognitive impairment. *Alzheimers Dement.* 2016;12:872-881.

65. Rubinski A, Frerich S, Malik R, et al. Polygenic effect on tau pathology progression in Alzheimer's disease. *Ann Neurol.* 2023;93: 819-829.

66. Chapuis J, Hansmannel F, Gistelinck M, et al. Increased expression of BIN1 mediates Alzheimer genetic risk by modulating tau pathology. *Mol Psychiatry.* 2013;18:1225-1234.

67. Franzmeier N, Rubinski A, Neitzel J, et al. The BIN1 rs744373 SNP is associated with increased tau-PET levels and impaired memory. *Nat Commun.* 2019;10:1766.

68. Franzmeier N, Ossenkoppele R, Brendel M, et al. The *BIN1* rs744373 Alzheimer's disease risk SNP is associated with faster Aβ-associated tau accumulation and cognitive decline. *Alzheimers Dement*. 2022;18:103-115.

69. Lee SH, Meilandt WJ, Xie L, et al. Trem2 restrains the enhancement of tau accumulation and neurodegeneration by β-amyloid pathology. *Neuron*. 2021;109:1283-1301.

70. Wood JI, Wong E, Joghee R, et al. Plaque contact and unimpaired *Trem2* is required for the microglial response to amyloid pathology. *Cell Rep*. 2022;41:111686.

71. Livingston G, Huntley J, Sommerlad A, et al. Dementia prevention, intervention, and care: 2020 report of the *Lancet* Commission. *Lancet*. 2020;396:413-446.

72. Young AL, Marinescu RV, Oxtoby NP, et al. Uncovering the heterogeneity and temporal complexity of neurodegenerative diseases with subtype and stage inference. *Nat Commun*. 2018;9:4273.

73. Vogel JW, Young AL, Oxtoby NP, et al. Four distinct trajectories of tau deposition identified in Alzheimer's disease. *Nat Med*. 2021;27:871-881.

74. Murray ME, Graff-Radford NR, Ross OA, Petersen RC, Duara R, Dickson DW. Neuropathologically defined subtypes of Alzheimer's disease with distinct clinical characteristics: A retrospective study. *Lancet Neurol*. 2011;10:785-796.

75. Graff-Radford J, Yong KXX, Apostolova LG, et al. New insights into atypical Alzheimer's disease in the era of biomarkers. *Lancet Neurol*. 2021;20:222-234.